Journal of Petroleum & Environmental Biotechnology
ISSN: 2157-7463
OPEN ACCESS Freely available online
Research Article

Successful Implementation of Artificial Intelligence and Machine Learning in Multiphase Flow Smart Proxy Modeling: Two Case Studies of Gas-Liquid and Gas-Solid CFD Models

Amir Ansari, S. Sina Hosseini Boosari*, Shahab D. Mohaghegh

Department of Petroleum and Natural Gas Engineering, West Virginia University, USA

ABSTRACT

It is almost impossible to solve the modern fluid flow problems without the use of Computational Fluid Dynamics (CFD). In petroleum industry, flow simulations assist engineers to develop the most efficient well design and it is essential to understand the multiphase flow details. However, despite the high accuracy, performing the numerical simulation fall short in providing the required results in timely manner. This article presents two case studies of Smart Proxy Models (SPM) utilizing artificial intelligence (AI) and Machine Learning (ML) techniques to appraise the behavior of the chaotic system and predict the dynamic features including pressure, velocity and the evolution of phase fraction within the process at each time-step at a much lower run time. Proposed cases concentrate on 2-D dam-break and 3-D fluidized bed problems, using OpenFOAM and MFiX, CFD software applications, respectively.

This paper focuses on building and improving the artificial neural network (ANN) models characterized by feed-forward back propagation method and Levenberg-Marquardt algorithm (LMA). Each case study contains multiple scenarios to gradually enhance the model capabilities to forecast the dynamic parameters. Results for both cases indicate that 8-10 hours of computational time for running CFD simulation, reduces to a few minutes when is done by developed AI-based models along with less than 10% error for entire process.

Keywords: Computational fluid dynamic; Fluid mechanic; Multiphase flow; Dynamic flow; Artificial neural network

Abbrevations: ρ: Density; μ: Dynamic Viscosity; g: Gravitational force; γ: Second Viscosity; U: Velocity; P: Pressure; τ: Diffusion Coefficient Over Density; γ: Phase Fraction; CFD: Computational Fluid Dynamics; SPM: Smart Proxy Model; AI: Artificial Intelligence; ANN: Artificial Neural Network; LMA: Levenberg-Marquardt Algorithm; RMSE: Root Mean Square Error

INTRODUCTION

Fluid mixtures such as oil and gas components, combined with solid particles as well as water, are produced constantly from the reservoirs. Multiphase production complexity, CO_2 capturing, CO_2 injection process, separation of mixture components, transportation by pipes and fluid flow in porous media are some of the multiphase flow example in petroleum scope [1,2]. Therefore, it is important in petroleum engineering to understand multiphase flow behaviors and how the details can be predicted [3].

Numerical-based multiphase flow simulation is a time-consuming process because of considering the simultaneous equations of many physical parameters. Therefore, proxy models help engineers to overcome this shortage by simplifying the physics and neglecting the complexities of the numerical models. On the other hand, ANN models, which are based on AI and ML, accurately replicate the functionalities of the system honoring dynamic nature of the problem in higher speed compared to numerical simulation. Another significant advantage of this technique is prediction of the fluid properties for unconventional reservoirs which requires special recovery operations due to the complexity and unique conditions [4].

In this article, two case studies have been conducted to evaluate the contribution of AI in CFD problems. Both proposed problems are two phase dynamic phenomena and the numerical simulations require sophisticated mathematical modeling. First case is gas-liquid interaction and is called “breaking of a dam”, while second case is gas-solid combination and is called “fluidized bed”.

Many studies have been conducted in unconventional reservoirs’

Correspondence to: Sina Hosseini Boosari S, Department of Petroleum and Natural Gas Engineering, West Virginia University, USA, Tel: +13044136683; E-mail: sehosseiniboosari@mix.wvu.edu

Received: January 28, 2020, **Accepted:** February 28, 2020, **Published:** March 06, 2020

Citation: Ansari A, Boosari SSH, Mohaghegh SD (2020) Successful Implementation of Artificial Intelligence and Machine Learning in Multiphase Flow Smart Proxy Modeling:Two Case Studies of Gas-Liquid and Gas-Solid CFD Models. J Pet Environ Biotechnol. 11:401. doi: 10.35248/2157-7463.20.11.401

topic from pore scale up to reservoir scales to improve the understanding of flow behavior and properties in complex unconventional formations [5]. One of the first use of AI in petroleum science goes back to 90's, which authors used ANN to design a model to predict the formation permeability [6]. Also Mohaghegh and Amery [7], calculated well performance index after hydraulic fracturing utilizing ANN. New correlation of estimating the crude oil viscosity has been achieved by using ANN model [8]. Sun and Durlofski [9] used principal component analysis considering data-spaced inversion process to forecast reservoir production. A combination of statistical and ML techniques were used by Satija et al. [10] to assess the reservoir performance without conducting history matching with optimum processing time. Classifying the wells with and without the liquid loading is another application of using unsupervised ML techniques in reservoir engineering [11].

MATERIALS AND METHODS

Generally, there are two different methods for multiphase flow numerical solution. The first method is Eulerian–Lagrangian and the second is Eulerian – Eulerian approach. Eulerian solution is based on the locations during the process by using Navier–Stokes equation and Lagrangian solution is based on particles movement during the process by considering newton's equation. Eulerian–Lagrangian method is the combination of both Eulerian and Lagrangian solutions, it means that continuous phase is considered for Eulerian and dispersed phase considered for Lagrangian solution, but in Eulerian–Eulerian approach for both phases, Eulerian solution will be used [12,13]. Table 1 shows different approaches with respect to the scale of the problem.

In order to solve CFD problems, two governing equations need to be solved, momentum and mass conservation.

For momentum conservation, Navier-Stokes equation is present as (Note that the fluid is considered as Newtonian incompressible fluid):

$$\frac{\partial \rho U}{\partial t}+\nabla.(\rho UU)-\nabla.\mu\nabla U-\rho g=-\nabla p \quad (1)$$

Where $(\partial \rho U)/\partial t$ is change of velocity with time, $\nabla.(\rho UU)$ is convective term, $\nabla.\mu\nabla U$ is velocity diffusion term, ρg is body force term, as external forces that act on the fluid (gravity), ∇p is pressure term, fluid flows in the direction of largest change in pressure.

In addition, for mass conservation, continuity equation is present as:

$$\frac{\partial \rho}{\partial t}+\nabla.(\rho U)=0 \quad (2)$$

Where U is velocity, ρ is density, p is pressure, μ is dynamic viscosity, and g is gravitational force. By involving volume of fluid technique and defining new term called γ which is phase fraction in one cell, the density as is mentioned before would be

$$\rho_m=\rho_1\gamma_1+\rho_2\gamma_2 \ \ \rho_m=\gamma\rho_1+\left(1-\gamma\right)\rho_2 \quad (3)$$

For viscosity

$$\mu_m=\mu_1\gamma_1+\mu_2\gamma_2 : \mu_m=\gamma\mu_1+\left(1-\gamma\right)\rho\mu_2 \quad (4)$$

Where, ρ_m is mixture density, ρ_1 is water density, ρ_2 is Air density, μ_m is mixture viscosity, μ_1 is water viscosity and μ_2 is Air viscosity.

γ could be any value between one and zero and this symbol represent the phase fraction in each computational cell. γ=1 means that, the cell is completely occupied by water and if it is filled with air, γ is zero. Generally, phase fraction equation is:

$$\gamma=\frac{\text{fluid volume}}{\text{cell volume}} \quad (5)$$

Another equation is transport equation (for property φ) with following general form:

$$\frac{\partial\left(\rho\varphi\right)}{\partial t}+\nabla.(\rho\varphi U)-\nabla.\left(\tau\nabla\varphi\right)=S\varphi \quad (6)$$

$\frac{\partial(\rho\varphi)}{\partial t}$ represents the rate of change of property φ with time, $\nabla.(\rho\varphi U)$ is advection of property φ by the fluid flow (net rate of flow-convection),also term $\nabla.(\tau\ \nabla\varphi)$ represents the rate of change due to diffusion of property φ. (τ is diffusion coefficient divided by the fluid density) and last term (S_φ) is the rate of change due to other source.

Transport equation with following form is used to calculate the relative volume fraction in each cell:

$$\frac{\partial\gamma}{\partial t}+\nabla.\ (\gamma U)=0 \quad (7)$$

By adding artificial compression term into this equation, necessary compression of the surface will be calculated:

$$\frac{\partial\gamma}{\partial t}+\nabla.\ (\gamma U)+\nabla.\left(\gamma\left(1-\gamma\right)\mu_r\right)=0 \quad (8)$$

Artificial neural network

Nowadays ANNs are being extensively used in many areas and different application from engineering to medical science and etc. [14]. A feedforward backpropagation method of training moves forward and computes the related values then this computed value is compared to the main value and based on the error calculation, it goes back in order to reduce the errors by modifying the weights. Levenberg–Marquardt algorithm (LMA) was selected for training process, LMA is known as the fastest algorithm for medium size

Table 1: Multiphase flow modeling approaches [14].

Name	Gas Phase	Solid Phase	Coupling	Scale
Discrete Bubble Model	Lagrangian	Eulerian	Drag Closure for bubbles	10 m
Two Fluid Model	Eulerian	Eulerian	Gas-Solid drag closure	1 m
Unresolved Discrete Particle Model	Eulerian	Lagrangian	Gas-particle drag closure	0.1 m
Resolved Discrete Particle Model	Eulerian	Lagrangian	Boundary condition at particle surface	0.01 m
Molecular Dynamics	Lagrangian	Lagrangian	Elastic collisions at particle surface	<0.001 m

of data and operates as an iterative procedure based on numeric minimization [15,16].

In order to evaluate the accuracy of ANN model, the cell-based error was defined as the absolute value of subtraction of CFD and NN. In addition, RMSE is used to assess the overall error.

$$Error = abs\left[\frac{\left(CFD_{value} - CFD_{valuemean}\right)}{\left(CFD_{valuemax} - CFD_{valuemin}\right)} - \frac{\left(Smart\ proxy_{value} - CFD_{valuemean}\right)}{\left(CFD_{valuemax} - CFD_{valuemin}\right)}\right] \times 100 \quad (9)$$

$$RMSE = \sqrt{\frac{1}{n}\sum_{j=1}^{n}\left(y_{CFD} - y_{NN}\right)^2} \quad (10)$$

The majority of data-set which includes 70% of the data, was used for learning in training part, 15% of the data-set was utilized for validation and 15% of the data-set was considered for testing part.

Deployment

There are two types of deployment; "Non-cascading" and "Cascading". First one refers to the type of deployment where the CFD data-set is fed to ANN model to predict the next time-step (Figure 1). In contrast, in "cascading" deployment, the input to the ANN is provided from predicted value in previous time-step. In other words, only one time-step from CFD software is required to initiate the deployment process and develop the results for rest of the time-steps (Figure 2). In this study, the steps to reach the best non-cascading model are presented. Providing a perfect non-cascading model with maximum precision and minimum error leads to acceptable cascading result [17,18].

To accomplish the objective of these two case studies, three different approaches are designated as following:

Approach 1: Using single time-step for training

Approach 2: Using multiple time-steps from significant dynamic moments for training

Approach 3: Involving time-steps with highest error in training system

Case Study 1

This case consists of a square tank with a column of water located behind a membrane on the left side (Figure 3a). At the beginning (t=0), the membrane drops and the column of liquid collapses. During the falling, the liquid hits the right wall of the tank and generates a complicated two-phase flow structure [19]. Each grid has a specific index, which indicates the location of the grid with distance from the walls.

Dependence of the parameters to each other and degree of the dependency plays a significant role in input determination. On the other hand, in order to build a comprehensive model, all potential assumptions that might be effective on physics of the problem should be considered. Four favorable variables are selected for this case including phase fraction, x-direction velocity, y-direction velocity and pressure.

24 inputs have been demarcated for training purposes, including: four variables for the focal cell, four variables for the distance of the focal cell from boundaries and four variables are considered

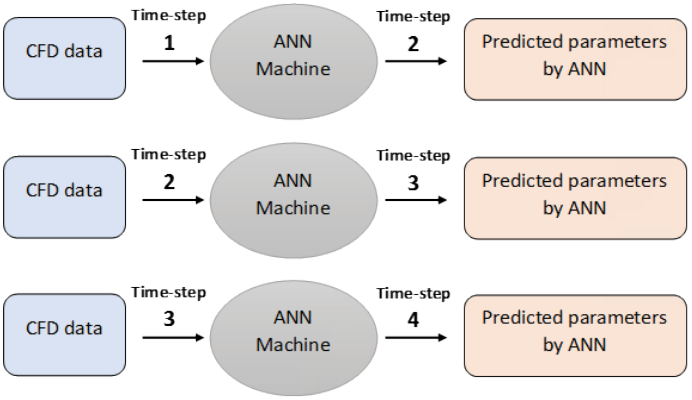

Figure 1: Non-cascading deployment workflow.

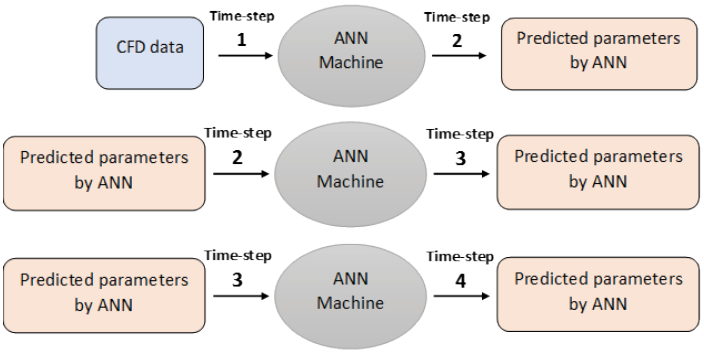

Figure 2: Cascading deployment workflow.

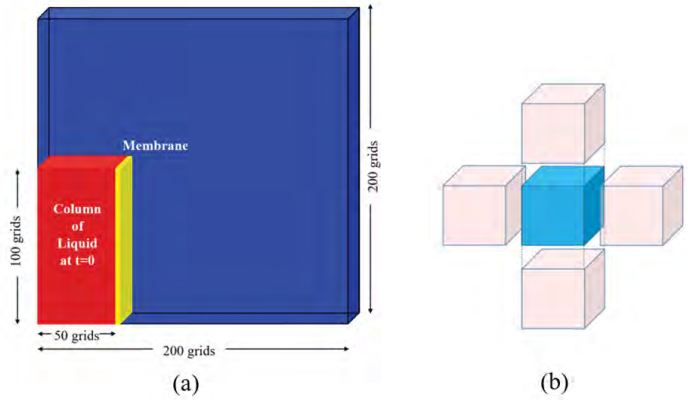

Figure 3: (a) Geometry and initial condition case study 1, (b) Neighbors of the focal cell in 2-D model.

for each neighbor cell (four cells surrounding the focal cell (Figure 3b) and the network is trained for each variable, separately. More details about data generating, time-step selection and training process are described in [20].

Three types of grid sizes are assessed in this case; "medium", "fine" and "very fine" containing 50, 200 and 400 grids in X and Y axes, respectively. Once the simulations were conducted, it was confirmed that the "fine" grid classification is the most appropriate mesh size for the problem's condition and the two other models were denied due to the low resolution and creating high number of records.

First approach: building the model using single time-step for training

In first step for building the ANN model, one time-step's data-set (2300 as the input and 2301 as the output of ANN) from CFD result

was selected to evaluate the capability of the model. Deployment result indicated that the model can't be trained properly with one time-step's data-set in entire process and after a couple of time-steps' successful prediction, the error increases.

For each variable, one ANN model is required including phase fraction, pressure, x-direction velocity and y-direction velocity and the correspond result is presented in the Figure 4 (the phase fraction result is presented as a sample for each approach The left, middle and right figures are representing CFD, ANN and error distribution, respectively. In error distribution figure, the red points represent at least 10% error.

In order to compare the predicted result by ANN model and visualize the performance, three plots were generated. The first plot on the left side is generated from CFD simulator, the middle one represents the prediction data performed by ANN and the right plot is the error percentage between CFD and ANN model.

Second approach: building the model using multiple time-steps from significant dynamic moments for training

In this approach, unlike the previous method, 16 time-steps data-set were selected from the most significant dynamic moments for training process. The involved time-steps with their respective real time are presented in Figure 5. One model was built for each parameter and the phase fraction result is shown in Figure 6. The results indicated that except for some time-steps the error distribution in entire process is less than 10%.

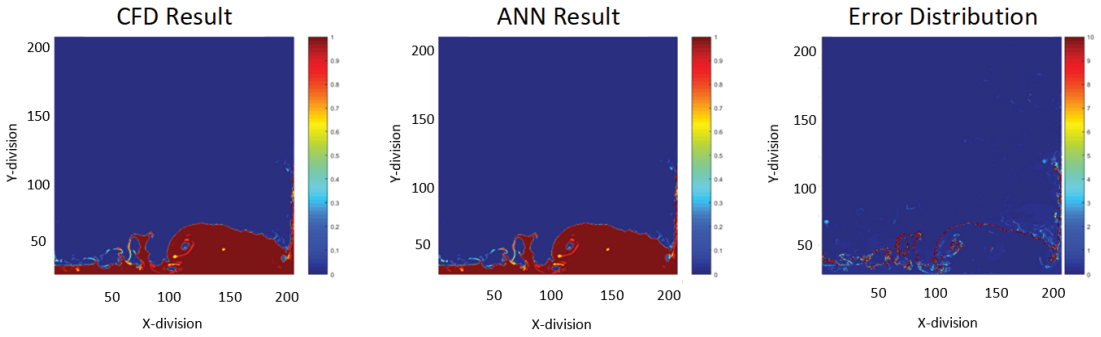

Figure 4: Phase fraction at time-step 2305 (five time-steps further).

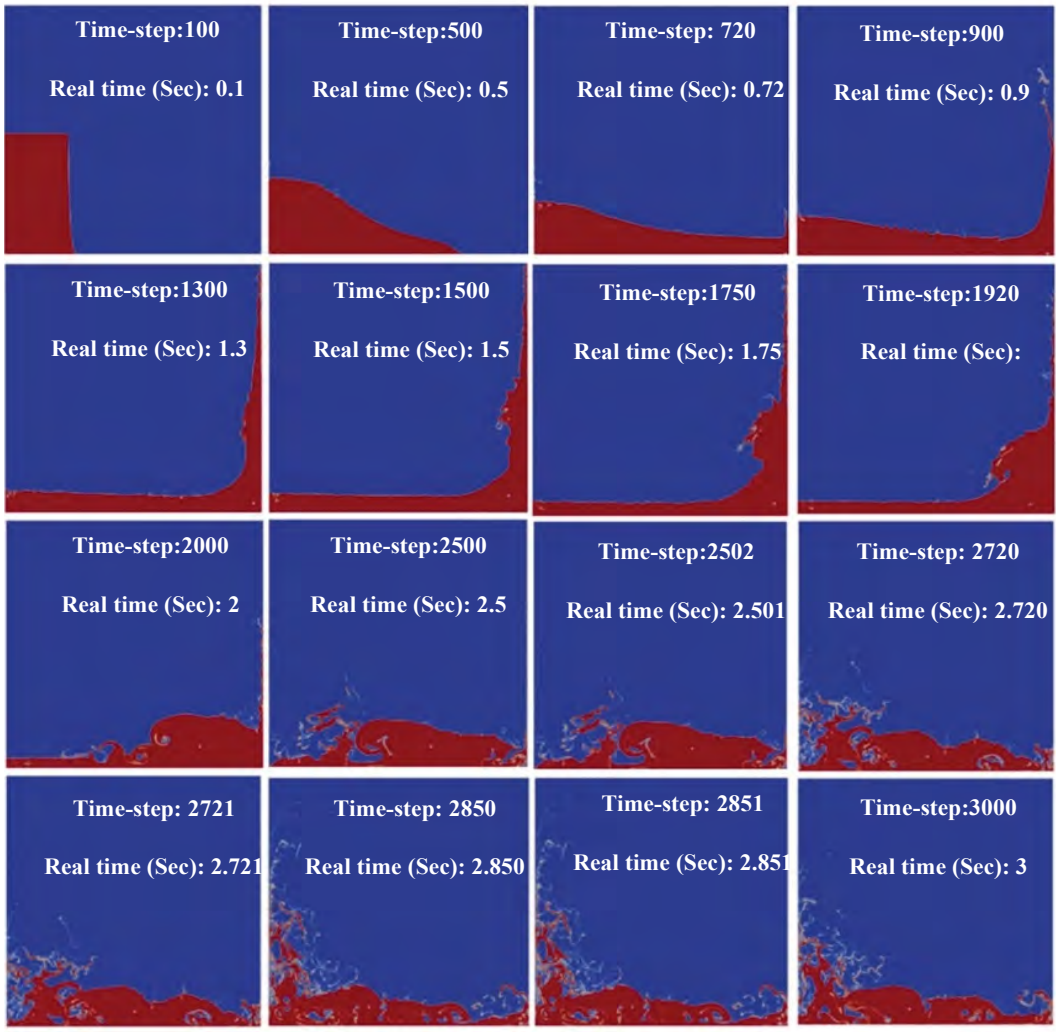

Figure 5: Significant dynamic moments used in the second approach with the real time.

Third approach: involving time-steps with highest error in training system

From previous section, using 16 time-steps for building the model, it was concluded that involving significant movements in the training process was a great enhancement to attain a comprehensive model. Furthermore, it was found out in some time-steps, particularly for pressure and velocity, more errors have been occurred. In order to improve the accuracy of each model, more time-steps from the moments with highest error were added to the training data-set. This consideration improved the non-cascading model significantly. The phase fraction result of this approach is presented in Figure 7.

The number of records for first, second and third approach was 40,000, 640,000, 1,200,000, respectively. The average RMSE of the entire process for second and third approach is presented in Figure 8. The maximum error for all parameters was less than 10% and it was occurred in time-step 520 for phase fraction.

Case Study 2

Case study 2 concentrates on a fluidized bed problem to show the capabilities of this method when it comes to three-dimensional gas-solid interactions. Figure 9a shows the geometry of this problem which is a rectangular fluidized bed with a square cross section. One-sixth of the fluidized bed is filled with sand which is initially at rest. The sand particles are perfect spheres with the density of 2000 kg/m^3. The initial volume fraction of gas is 0.42. The inlet air velocity is set to 0.6 m/s which is uniformly distributed in the upward direction. The air discharges into atmospheric pressure up on top of the bed.

As air is injected into the bed, at first, large gas pockets form that cause the sand particles to move upward as a slug. In matter of few seconds, the gas pockets break up, leading to the breakup of sand slugs, which shower back down. At this time, air enters the bed and forms bubbles, which moves up through the sand bed, leading to the fluidization of the sand particles. The output attributes of the numerical simulator used in this case study are; gas volume fraction, gas pressure, solid pressure, velocity of gas in x direction, velocity of gas in y direction, velocity of gas in z direction, velocity of solid in x direction, velocity of solid in y direction and velocity of solid in z direction [21].

This problem is three dimensional and each cell is in contact with 28 neighbor cells; 6 of them have the surface contact with the focal cell which have high correlation with the focal cell. The dynamic property of these 6 cells were included in the model preparation process in order to fully capture the spatial relationship between all dynamic features. Figure 9b shows the focal cell and its 6 neighbor cells.

It is also crucial to teach ANN where the cell is located and how far it is from the boundaries to learn the spatial correlation between different parameters. Also, like case study 1, wall has a significant impact on the flow pattern and its location should be included in the ANN training. Six different distances to the wall confinements (top, bottom, east, west, north, and south) are considered to define the exact location of each cell and parameters associated with each cell [22].

First approach: building the model using single time-step for training

ANN can have either one output at the same time or multiple outputs. Having multiple outputs simultaneously increases the training time and the network has to fit multiple outputs with the same weights, so the network has less flexibility to learn from data but sometimes it gives a better result especially when there is a correlation between the outputs.

Time-step 100 was used as input alone with time-step 101 as the

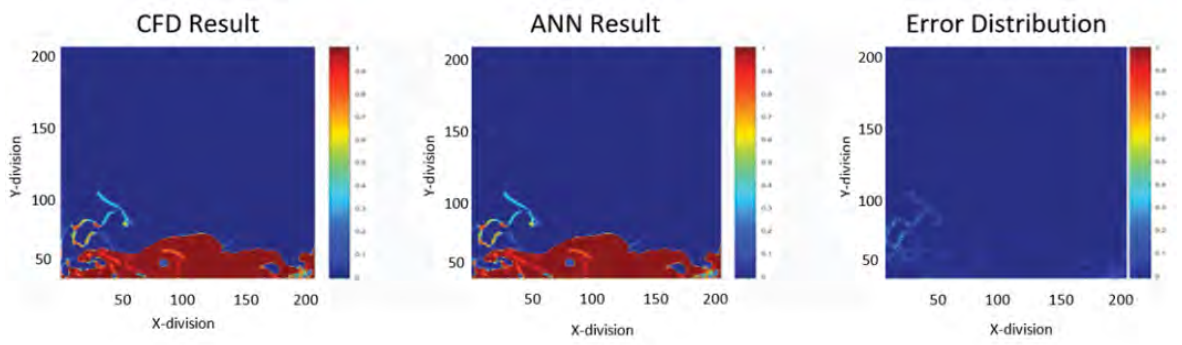

Figure 6: Phase fraction, the maximum error in whole process time-step at 2660.

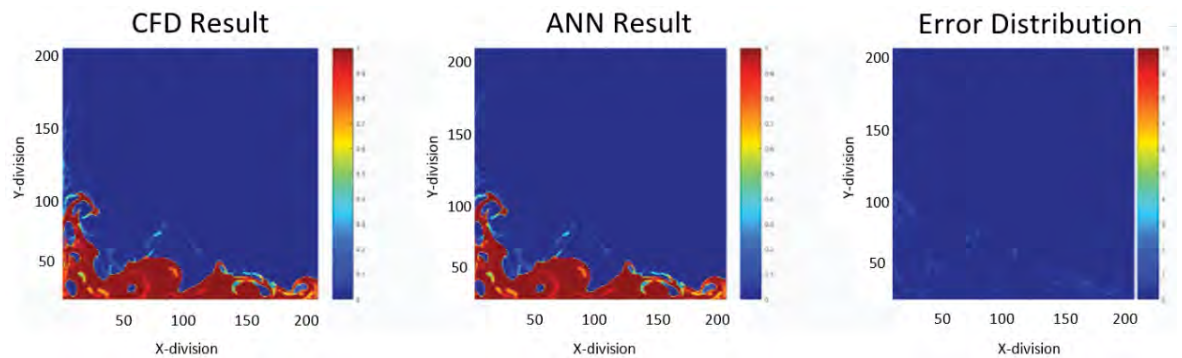

Figure 7: Phase fraction, the maximum error in whole process.

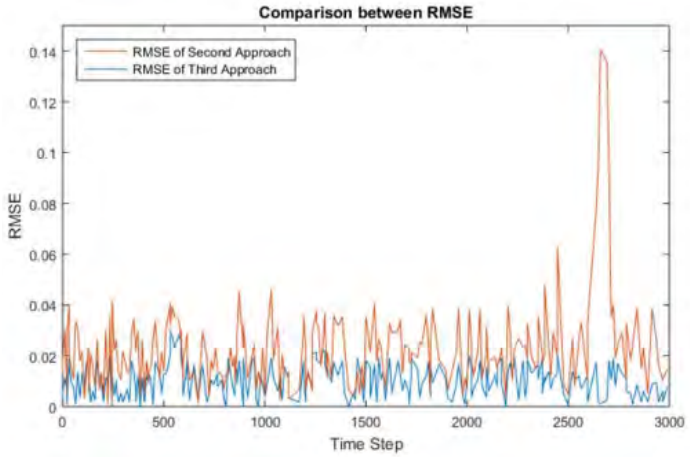

Figure 8: Phase fraction RMSE distribution over time for second and third approach.

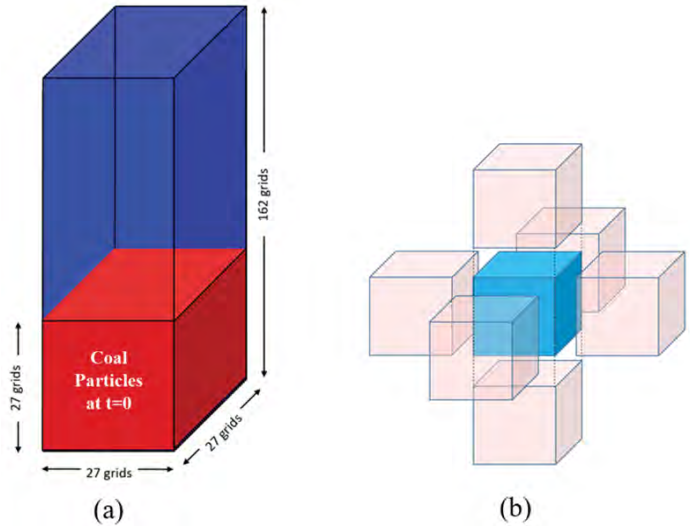

Figure 9: (a) Geometry and initial condition case study 2, (b) Neighbors of the focal cell in 3-D model.

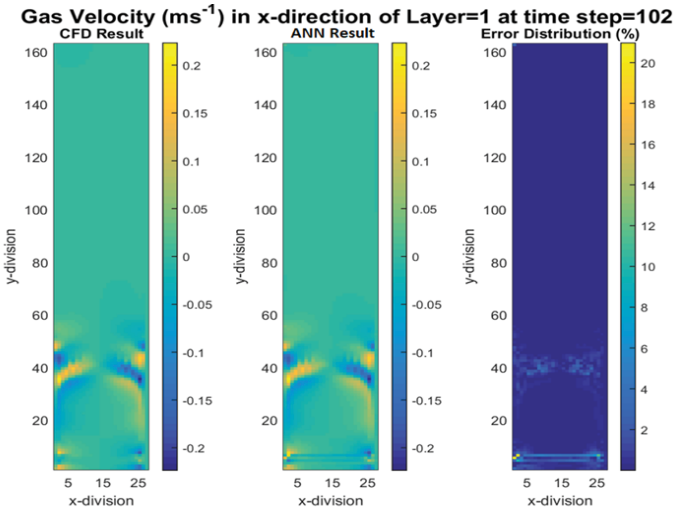

Figure 10: Gas x-velocity of time-step 102 for layer one (z=1).

output. The ANN was trained successfully and the time-step 102 was predicted, the time-step that ANN has never seen before. The results of the ANN model versus CFD for gas velocity are shown in the next figures. As it is shown in Figure 10, ANN model is able to replicate the MFIX simulation results that show gas velocity (x-direction) distribution at time-step 102 for layer one. The maximum prediction error occurred occasionally at some points with the value less than 21% while we see an error near to zero in the rest of the domain.

Similar results have been obtained for gas velocity y-direction where the maximum prediction error occurred occasionally with the value less than 25% (Figure 11).

As an alternative, it is decided to have three components of gas velocity as the outputs of the ANN at the same time, because of existing the potential correlation among the gas velocity components.

As another advantage of this approach, it should be stated that having multiple outputs at the same time would reduce the number of neural networks models. There are total of nine different ANN needed for deployment, this number could be reduced to three if each network has three outputs simultaneously.

Figure 12 shows the results of ANN model and comparison with CFD simulation results. Fairly good results were obtained (Only the lower section of the fluidized bed is shown in the figure for better resolution). Gas velocity in the y-direction contains the highest error, which is less than 20% at some single points, but

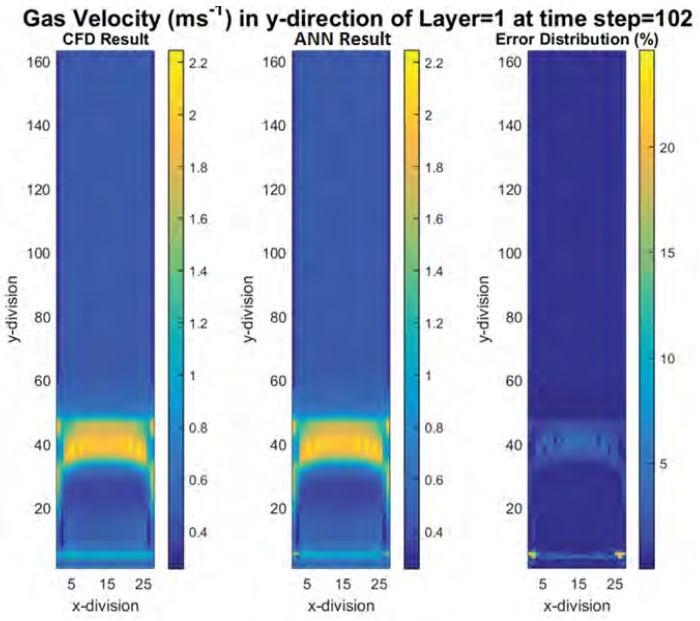

Figure 11: Gas y-velocity of time-step 102 for layer one (z=1).

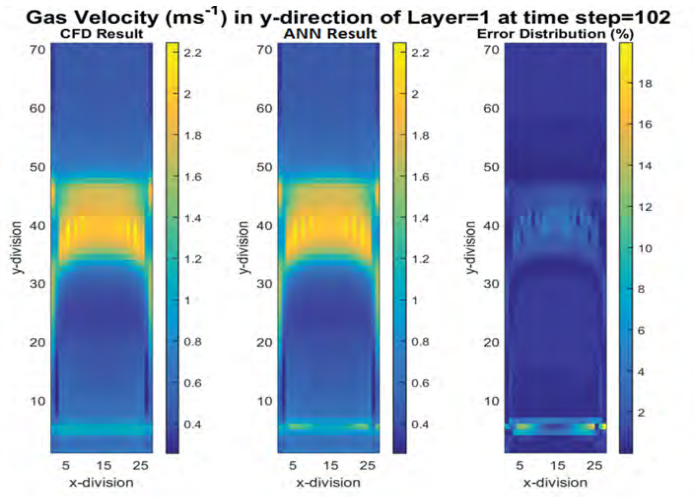

Figure 12: Gas y-velocity of time-step 102 for layer one (z=1).

the rest of the domain have negligible errors. This new approach enhanced the results by 5% when it compares to the single output approach (Figure 11).

Using multiple output at the same time improved the results, however, it needed more pre-processing and processing time. Therefore, for the following approaches, single output will be presented.

Second approach: building the model using multiple time-steps from significant dynamic moments for training

The technique outline so far uses a single time-step for input and output of the ANN. However, the gas-solid flow undergoes a regime change, from a slugging flow at the beginning to a fluidized regime as time goes by. The ANN trained with the data from when the flow field is slugging does not have the predictive capability of capturing the flow dynamics, when the bed is fully fluidized. In order to train an ANN model, containing wider range of applicability, the input and output of the ANN must be trained on data from multiple time-steps, capturing many changes taking place in the flow.

Figure 13 shows three different time-steps involved in the training process. These time-steps were selected from the significant dynamic moments of the problem, when the flow is slugging at first (time-step of 200), then transitioning (time-step 1000) and finally fluidizing stage (time-step 4000). One more parameter was added to the training data-set that shows the actual elapsed time for each time-step. Figure 13 shows the gas volume fraction contours in the CFD simulations at time-steps 200 (0.2 sec elapsed time), 1000 (1 sec elapsed time) and 4000 (4 sec elapsed time).

Time-steps 200-202, 1000-1002, and 4000-4002 have been used for the training. The deployment process is then conducted with the trained ANN by inputting time-step 200 all the way to time-step 4000 (non-cascading approach). The results are presented in terms of RMSE of gas volume fraction in Figure 14. Clearly in the time-steps that we included training data; the amount of error is minimum (Blue line).

Third approach: building the model using multiple time-step and single Output

Similar to the case study 1, the time-steps with larger amount of errors in second approach to the need for additional ANN training at those time-steps (potentially other dynamic behaviors are taking place in the bed, requiring additional training). The contour plot of gas volume fraction at time-step 500, where the RMSE is high (blue line) is shown in Figure 15. It is clear that at around this time-step, flow is transitioning from the initial plug flow behavior to a more bubbling flow. This change in the flow regime is not properly captured, since the input data to ANN at the training stage did not include any data from the time-steps, when transitioning is taking place.

Figures 14 and 15 show a decrease in RMSE, when data from time-steps where RMSE peeks in second approach were added to the training data-set. Although the RMSE is very low in non-cascading approach for all the times-steps, using the same ANN model in cascading mode will be accompanied by a large error. This study showed that the ANN model could be a viable tool for predicting gas-solid flow behavior in a fluidized bed. However, to make the trained ANN more general, the cascading deployment

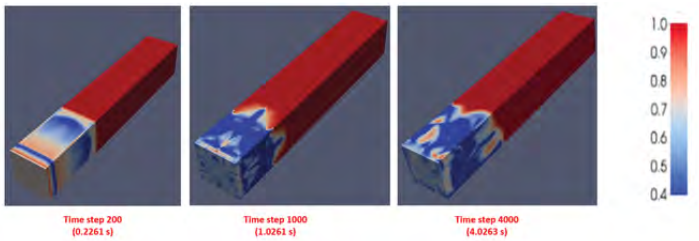

Figure 13: Significant dynamic moments used in the second approach.

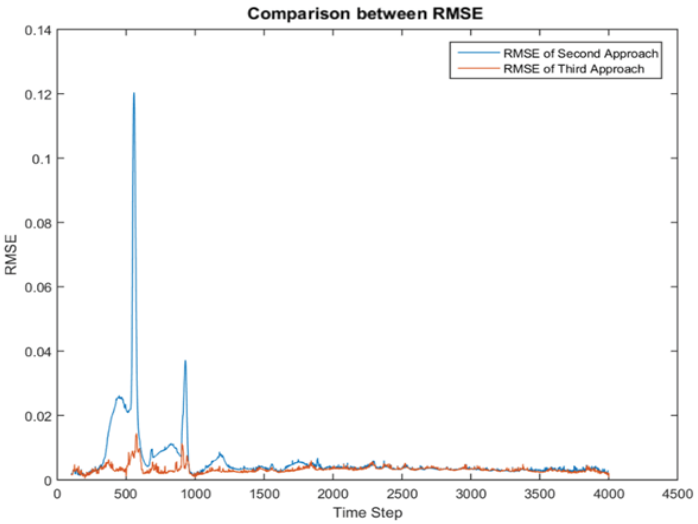

Figure 14: Gas fraction RMSE distribution over time for second and third approach.

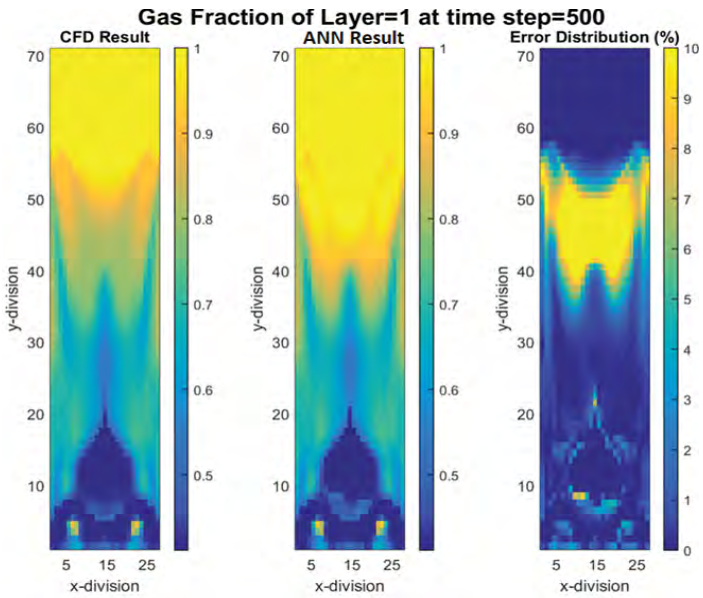

Figure 15: Gas fraction of time-step 500 for layer one (z=1).

needs further research and more parameters should be considered in order to minimize the error propagation over the time.

DISCUSSION AND CONCLUSION

In this paper, two case studies, "Dam-break" and "Fluidized bed", have been conducted to demonstrate the successful implementation of Artificial Intelligence and Machine Learning in multiphase flow field of study. The main objective of this research was forecasting the behavior of the fluid flow parameters with acceptable precision in comparison with CFD simulator result. Moreover, proposed

approach will significantly reduce the computational cost of optimization process compared to CFD simulator since this process requires multiple runs. Results indicated that the ANN model was able to predict the behavior of the fluid with satisfactory results. In addition, processing time has been altered from hours to minutes scale.

REFERENCES

1. Pope GA. The application of fractional flow theory to enhanced oil recovery. Soc Pet Eng J. 1980;20:191-205.
2. Alabboodi MJ, Mohaghegh SD. SPE-184064-MS conditioning the estimating ultimate recovery of shale wells to reservoir and completion parameters, 2016.
3. Boosari SSH, Aybar U, Eshkalak MO. Carbon dioxide storage and sequestration in unconventional shale reservoirs. J Geosci Environ Prot. 2015;3:7–15.
4. Esmaili S, Kalantari-Dahaghi A, Mohaghegh SD. Forecasting, sensitivity and economic analysis of hydrocarbon production from shale plays using artificial intelligence & data mining. SPE Can. Unconv Resour Conf. 2012:1–9.
5. Boosari SSH, Aybar U, Eshkalak MO. Unconventional resource's production under desorption-induced effects. Petroleum. 2016;2:148-155.
6. Sgher M, El-Aminian K, Ameri S. The impact of stress on propped fracture conductivity and gas recovery in Marcellus Shale, 2018.
7. Mohaghegh S, Arefi R, Ameri S, Rose D. Design and development of an artificial neural network for estimation of formation permeability in Proceedings - Petroleum Computer Conference, 1994.
8. Naseri A, Yousefi SH, Sanaei A, Gharesheikhlou AA. A neural network model and an updated correlation for estimation of dead crude oil viscosity. Brazilian J Pet Gas. 2012;6: 31-41.
9. Sun W, Durlofsky LJ. A new data-space inversion procedure for efficient uncertainty quantification in subsurface flow problems. Math Geosci. 2017;49: 679-715.
10. Satija A, Scheidt C, Li L, Caers J. Direct forecasting of reservoir performance using production data without history matching. Comput Geosci. 2017;21:315-333.
11. Ansari A, Fathi E, Belyadi F, Takbiri-Borujeni A, Belyadi H. Data-based smart model for real time liquid loading diagnostics in marcellus shale via machine learning. SPE Canada. Unconv Resour Conf. 2018.
12. Biscarini C, Di Francesco S, Manciola P. CFD modelling approach for dam break flow studies. Hydrol Earth Syst Sci. 2010;14:705-718.
13. Van Der Hoef MA, Annaland MVS, Deen NG, Kuipers JAM. Numerical simulation of dense gas-solid fluidized beds : A multiscale modeling strategy. Annu Rev Fluid Mech. 2008;40:47-70.
14. Amato F, López A, Peña-Méndez EM, Vallhara P, Hampl A, Havel J. Artificial neural networks in medical diagnosis. J Appl Biomed. 2013;11:47-58.
15. Madsen K, Nielsen HB. Introduction to optimization and data fitting, 2008.
16. Hagan MT, Menhaj MB. Training feedforward networks with the Marquardt algorithm. IEEE Trans. Neural Networks. 1994;5:989-993.
17. Boosari SSH. Predicting the dynamic parameters of multiphase intelligence-(Cascading Deployment). Fluids. 2019;4:44.
18. Ansari A, Mohaghegh SD, Shahnam M, Dietiker JF. Modeling average pressure and volume fraction of a fluidized bed using data-driven smart proxy. Fluids. 2019;4:123.
19. Higuera P, Lara JL, Losada IJ. Three-dimensional interaction of waves and porous coastal structures using OpenFOAM®. Part I: Formulation and validation. Coast Eng. 2014;83:243-258.
20. Boosari SSH. Developing a smart proxy for predicting the fluid dynamic in DamBreak flow simulation by using Artificial Intelligence, West Virginia University, USA, 2017.
21. Ansari A. Developing a smart proxy for fluidized bed using machine learning, West Virginia University, USA, 2016.
22. Ansari A, Mohaghegh S, Shahnam M, Dietiker JF, Li T, Gel A. Data driven smart proxy for CFD application of big data analytics & machine learning in computational fluid dynamics, Part Three: Model building at the layer level; NETL-PUB-21860; NETL Technical Report Series; U.S. Department of Energy, National Energy Technology Laboratory: Morgantown, West Virginia, USA, 2018.